

A study on motion of machine tools' hexapod table on freeform surfaces with circular interpolation

Mohammad Reza Chalak Qazani ·
Siamak Pedrammehr · Mohammad Javad Nategh

Received: 26 June 2013 / Accepted: 10 August 2014 / Published online: 29 August 2014
© Springer-Verlag London 2014

Abstract Accuracy is greatly affected by nonlinear motion of hexapods. This need is more obvious when these mechanisms are used in machining environments where precision and surface qualities are of critical importance. In this paper, comprehensive algorithm for hexapod tool path programming is developed. Using C#.Net, this algorithm is developed based on circular motion and rotation of the table which has the capability of checking nonlinear error and keeping it in a controlled limit as well. Improved Tustin algorithm is used for interpolating circular path. To evaluate the accuracy of the developed algorithm on a freeform surface, a turbine blade is scanned, and its CAD model is developed. Taking zigzag strategies, movement on turbine blade surface is approximated with smaller circles using the algorithm presented in this paper. The output accuracy resulted from interpolation algorithm for passing on turbine blade surface is studied in SimMechanics of MATLAB software. Using Total Station camera, motion path of two turbine blades with different radius curves on the hexapod table is experimentally obtained. Finally, it can be stated that the developed algorithm based on circular interpolation has the capabilities of motion on freeform curves.

Keywords Hexapod · Tool path programming · Improved Tustin approach · Nonlinear error · Freeform surface

1 Introduction

The general demand on the machine tool design for high-speed machining lies primarily in the high acceleration capability of the machine axes while, at the same time, meeting the high demands on machining accuracy [1]. Currently, most of the machine tools are designed on basis of using simple open kinematic chain. Such multi-axis machines suffer from the disadvantage that each axis must either move or carry all other axes that are situated further along the kinematic chain. In order to overcome this weakness, parallel mechanism has found extensive application as the table or spindle of machine tools [2–4]. The accuracy is among the primary requirements for precision machining. This needs a thorough understanding of the tool path programming [5–7]. The purpose of the present study is to partially meet this need and fill the gap existing in the literature in this respect.

Dasgupta and Mruthyunjaya [8] developed an algorithm for singularity-free path planning of the Stewart platform manipulator. The limitations of their algorithm were its lack of confidence in detecting the nonexistence of a singularity-free path and its sensitivity to intersections of singularity hypersurfaces. Shaw and Chen [9] investigated an algorithm for generating the cutting path of a Stewart platform-based milling machine. Iso-scallop method and genetic algorithm are utilized respectively in the process of generating the cutting path and finding the configurations of the tool without a singular position in their research work. Merlet [10] investigated trajectory verification for a classical Gough-Stewart platform. In his study, the real-time method has been developed and errors have been controlled. Pugazhenthil et al. [11] developed an optimal trajectory planning algorithm for the hexapod machine tool during contour machining. They developed a code to maximize the stiffness of the structure and minimize the force requirement of the actuator, and the constraints of workplace and singularity have been taken into

M. R. Chalak Qazani (✉) · M. J. Nategh
Faculty of Technology and Engineering, Department of Mechanical Engineering, Tarbiat Modares University, Tehran, Iran
e-mail: m.r.chalakqazani@gmail.com

S. Pedrammehr
Faculty of Engineering and Natural Sciences, Sabanci University,
Tuzla, Istanbul, Turkey

account in their study. Peidong and Changlin [12] presented a new approach of motion planning based on the planned trajectory on a parallel kinematic machine. Their approach was verified by simulation results, which were consistent with the planned trajectory. Dash et al. [13] presented a numerical technique for path planning within the workspace of parallel manipulators. Isolated singularities have been eliminated through local routing method based on Grassmann's line geometry in their study. Afroun et al. [14, 15] presented a technique for generating optimal motion for a parallel delta robot and Gough parallel robot. In their study, the sequential programming quadratic method has been applied to find the optimal position of the spline control points. Harib et al. [16] developed an analytical model for trajectory planning of a redundant hybrid machine tool structure consisting of a Stewart platform and a two-degree-of-freedom rotary tilting table. Having presented eight coordinates, they defined five coordinates through conventional part programming and other three coordinates via trajectory planning. Li [17] investigated reconfiguration and tool path planning of hexapod machine tools. In his study, appropriate trajectory planning is considered to reduce nonlinear error in the path. Jinsong [18] utilized kinematic nonlinearity of parallel machine tools to investigate their interpolation accuracy. Zheng [19] developed a path control algorithm for a parallel machine tool and applied it to the CNC system software. The developed algorithm has been verified by machining experiments. Chalak Qazani et al. [20, 21] introduced hexarot mechanism as a novel 6-DOF parallel manipulator and investigated its nonlinear error using image processing technique. The effective parameters on nonlinear motion error of hexarot have also been determined in their study.

The purpose of this study is to add different kinds of circular interpolation with rotation of the table to interpolator unit of hexapod table, as to provide the table with capability of moving on freeform with approximation to smaller circles. Using mid-oscillating circle, nonlinear error of the motion of table is obtained. If the error rate becomes greater than the specified amount, the developed algorithm decreases the nonlinear error by decreasing the feed rate. In addition, this algorithm makes use of machine table with 2.5 degrees of freedom by controlling the rotation of table within its workspace. The output of the algorithm for motion on two different turbine blade surfaces with different radiuses is investigated by simulation in MATLAB software, and motion errors are obtained. By path programming, motion error is sensed and checked using Total Station camera.

2 Description of hexapod table

The mechanical prototype of a hexapod table developed for FP4M CNC milling machines and machining centers is shown

in Fig. 1. It consists of a moving platform accommodating the workpiece to be machined, a stationary platform fixed to the foundation and six pods, the upper ends of which are connected to the moving platform through six spherical joints and the lower ends are connected to the stationary platform through six universal joints.

3 Nonlinear error analysis of the hexapod table motion

In order to control error in an acceptable range, the value of nonlinear error must be obtained. Here, in this research, mid-oscillating circle is utilized to obtain the kinematic error.

Oscillating circle of a curve abuts the curve at a point. In other words, it has the same tangent and curvature as the curve has at that point. Just as the tangent line is the best line for approximating a curve at a given point, the oscillating circle is the best circle that approximates the curve at a point. The radius of the osculating circle is simply the inverse of curvature. This, however, is of critical importance both in nonlinear motion of the table and its path programming.

Curvatures vary throughout the whole path, and the radiuses of the oscillating circles at start and end points of the path are different. Therefore, the radius of the mid-oscillating circle is taken into account in this research (Fig. 2).

The normal vector of the plane consisting mid-oscillating circle, h , can be presented as follows:

$$h = P \times N = \begin{bmatrix} i & j & k \\ P_x & P_y & P_z \\ N_x & N_y & N_z \end{bmatrix} \quad (1)$$

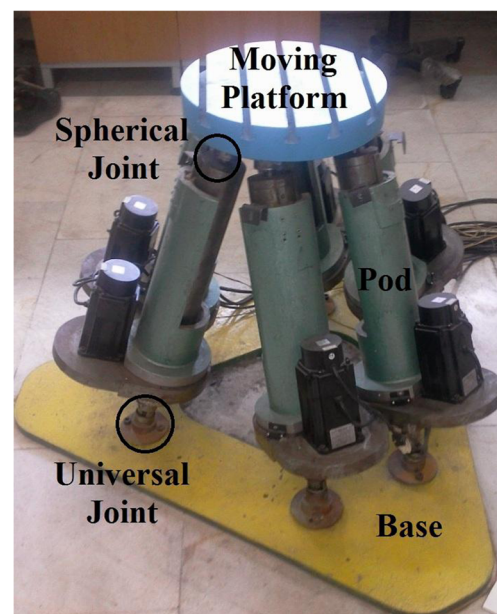


Fig. 1 The hexapod table

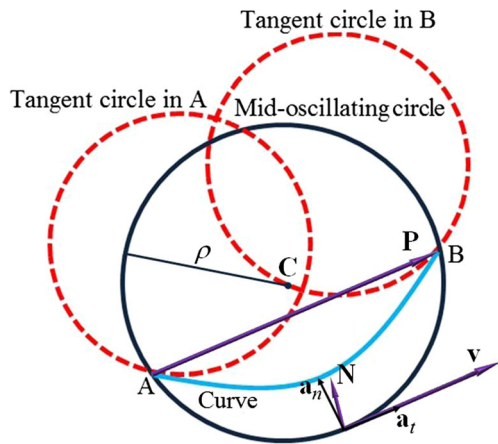


Fig. 2 Real and suitable paths

where P is the vector connecting two interpolated points A and B and N is the unit vector which is normal to the tangent vector. N can be obtained as follows:

$$N = a / |a \times v| \tag{2}$$

in which v and $a = a_t + a_n$ are respectively the linear velocity and acceleration vectors of the moving platform between A and B (see Fig. 2).

Since points A and B are in the plane with normal vector h , the center of the circular path can be obtained by solving the system of nonlinear equations as follows:

$$\begin{cases} (P'_x - C_x)^2 + (P'_y - C_y)^2 + (P'_z - C_z)^2 = \rho^2 \\ (P''_x - C_x)^2 + (P''_y - C_y)^2 + (P''_z - C_z)^2 = \rho^2 \\ h_x(C_x - P_x) + h_y(C_y - P_y) + h_z(C_z - P_z) = 0 \end{cases} \tag{3}$$

where $P' = (P'_x, P'_y, P'_z)$ and $P'' = (P''_x, P''_y, P''_z)$ are respectively position vectors of the points A and B , and $C = (C_x, C_y, C_z)$ is the center of the mid-oscillating circle. ρ is the radius of the mid-oscillating circle and can be obtained as follows:

$$\rho = (\rho_A + \rho_B) / 2 \tag{4}$$

ρ_A and ρ_B are respectively the radius of the oscillating circle at points A and B and can be defined as follows:

$$\rho_A = 1 / \kappa_A \tag{5}$$

$$\rho_B = 1 / \kappa_B \tag{6}$$

where κ_A and κ_B are curvatures in points A and B , respectively. Curvature in these two points can be determined by kinematics of pods and platform [22].

Considering direct kinematic equations [22] and substituting Eq. (3) into Eqs. (5) and (6), kinematic error equation can be written as follows:

$$e = \rho - \sqrt{\rho^2 - (S/2)^2} \tag{7}$$

In Eq. (7), S is the distance between two interpolated points A and B (i.e., the proper path), and it can be obtained in terms of operator-defined feed rate, F , and the time at which the control system responds to the servo motors, T_s , which yields the following:

$$S = F T_s \tag{8}$$

The maximum angular displacement between two interpolated points in terms of maximum nonlinear error, β , can be obtained as follows:

$$\beta = \text{tg}^{-1}(e/2R) \tag{9}$$

where R (mm) is the radius of the interpolated circle.

Linear velocity and acceleration of the j^{th} pod in the i^{th} position, l_j^i and $l_j''^i$, can be obtained solving the inverse kinematic problem of the mechanism [23–26], which can be expressed as follows:

$$l_j^i = (l_j^{i-1} - l_j^i) / T_s \tag{10}$$

$$l_j''^i = (l_j^{i-1} - l_j^i) / T_s \tag{11}$$

By having the length and linear velocities and accelerations of the pods, acceleration of the center of the moving platform

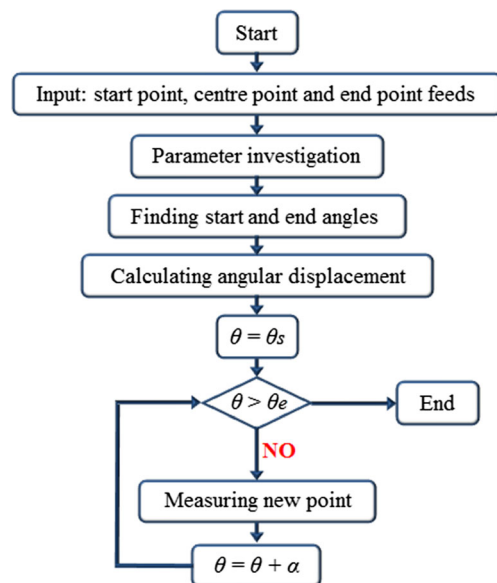


Fig. 3 Boundary conditions of 0.05-mm Tustin error and 0.25-mm nonlinear error

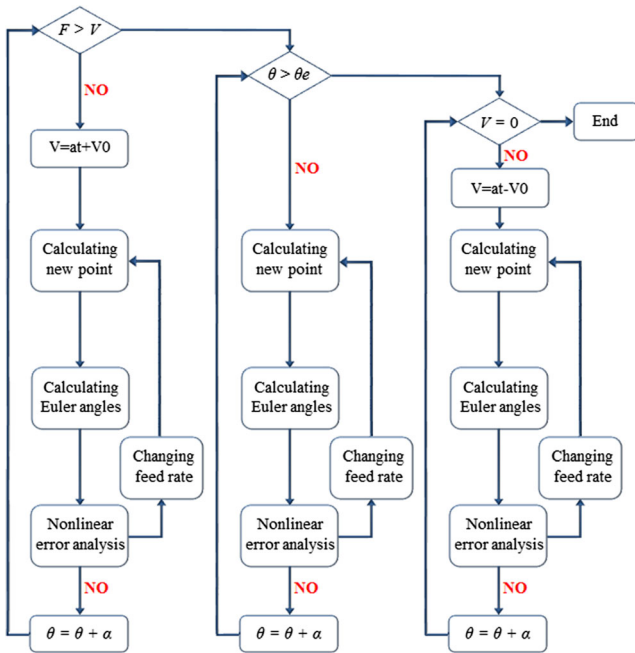


Fig. 4 Clockwise circular motion algorithm of hexapod table

can be calculated [22]. Substituting these data into Eqs. (2), (5), and (6) gives the curvature and the radius of oscillating circle. If kinematic error exceeds acceptable range, S has to be mitigated. In this condition, changing feed rate is of key importance in controlling the path length and kinematic error and can be obtained using the following:

$$F = 2\sqrt{2\rho e_{all} - e_{all}^2}/T_s \tag{12}$$

where e_{all} is the maximum allowed error. The developed CNC code, in order to control error in acceptable range, calculates the feed rate from Eq. (12) and replaces it with the previous one and then begins other interpolation process based on the new feed rate.

There are two main error sources in circular interpolation of hexapod table: One is nonlinear error which is considered to be 0.25 mm at maximum, and other is Tustin error with 0.05-

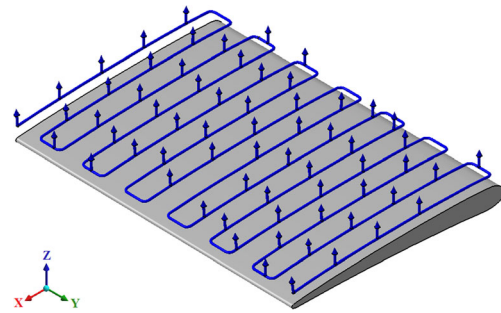


Fig. 6 Turbine blade with low curvature

mm maximum allowance. These allowances, however, are assumed considering the accuracy of the utilized measurement system (i.e., image processing).

Considering improved Tustin algorithm, the maximum angular displacement between two interpolated points, α , can be obtained as follows:

$$\alpha = \sqrt{16/(R-1)} = 4/\sqrt{R} \tag{13}$$

In Eq. (13), R is the radius of the interpolated circle, and it is in basic length unit (BLU) terms.

Considering $T_s=0.1$ (s), Eq. (12) can be rewritten compactly as follows:

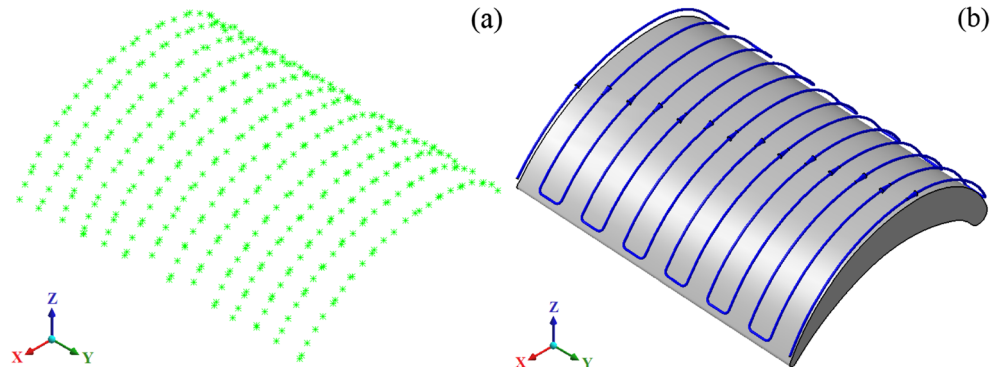
$$F = 4\sqrt{R}/T_s \tag{14}$$

In order to make use of rotational capability of machine table and to provide a motion with 2.5 degrees of freedom, table rotation must be considered while interpolation. For this purpose, to obtain Euler angles by the normal vectors of platform, the following relations are utilized:

$$\begin{aligned} A &= \text{Sin}^{-1}\left(n_y/\sqrt{n_y^2 + n_z^2}\right) \\ B &= \text{Sin}^{-1}\left(n_x/\sqrt{n_x^2 + n_z^2}\right) \\ C &= \text{Sin}^{-1}\left(n_x/\sqrt{n_x^2 + n_y^2}\right) \end{aligned} \tag{15}$$

In relation (15), A , B , and C angles present platform angle with respect to X , Y , and Z axes, respectively.

Fig. 5 a Turbine blade cloud of points. b CAD model created from cloud of points in CATIA and zigzag strategy display



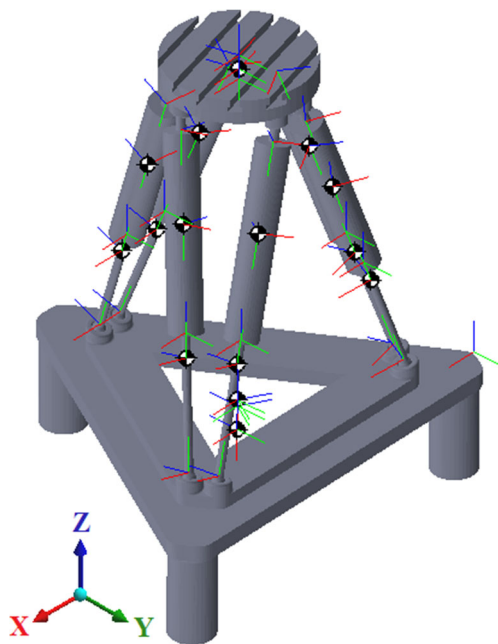


Fig. 7 Simulink model of hexapod table

4 Circular interpolation algorithm

Tool path programming for machine tools' hexapod table is developed based on circular interpolation. The main purpose of this research is to add different kinds of circular interpolators to the hexapod interpolator unit, in a way that would able to track the freeform path by dividing it to smaller circles and also by using circular interpolation and lining up the normal vector of the table to the radius of related circle. It should be noted that, while interpolating turbine blade surface with smaller circles, interpolator unit checks the nonlinear error and keeps it in controllable range.

There are two standards for using G-code in circular motion: One is using I and J parameters which define the geometry center of the moving platform according to its initial point, and the other method is utilizing circle radius (CR) parameter which specifies the radius of the circle [27].

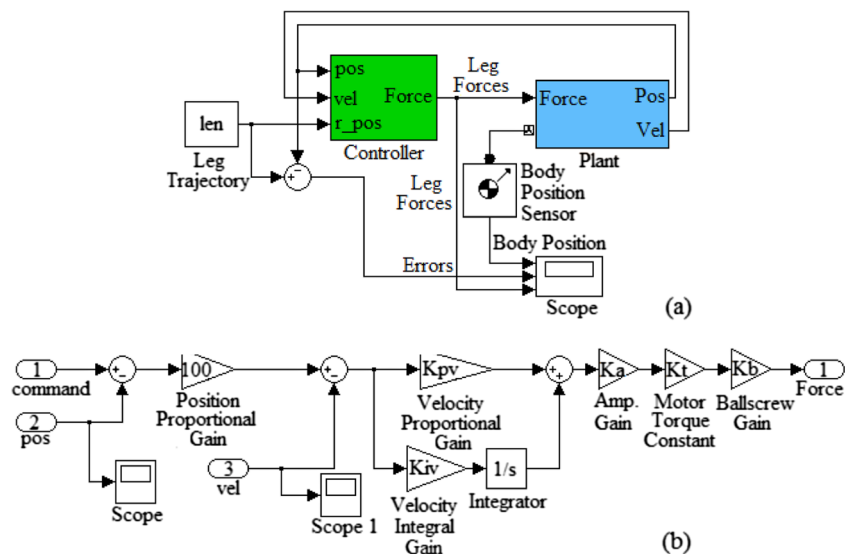
In the second method, if CR is positive, the angular motion of the circle will be lower than 180°, and vice versa. Figure 3 presents the developed algorithm for clockwise circular motion of the hexapod table.

The first step in Fig. 3 includes the following: start point of circular motion which is determined by existed position of tool, end point of circular motion which is determined by defined parameters in the same command, and circle center which is determined after primary calculations and independent from determining method. Using these parameters, the circle is determined and interpolation process is performed as well.

The second step is to verify input data. Since the operator may make a mistake in setting the parameters associated with the circle, program is able to check the parameters in this step. If the parameters associated with the circle are not verified, a message will be sent to the operator to check and modify the parameters. First, circle's radius is obtained for the start and end points of circular motion. By comparing the two numbers, if their absolute difference is greater than 0.05 mm, the error message will appear. Consideration of 0.05-mm difference for these two numbers is due to the numerical solution which is carried out by the algorithm.

The third step is associated with start and end angles of the circle. To perform more speedy interpolation and also to reduce the amount of computation, machine's center point is transferred to the circle center using a matrix. Considering

Fig. 8 a Motion simulation of hexapod. b Hexapod control system in SimMechanics



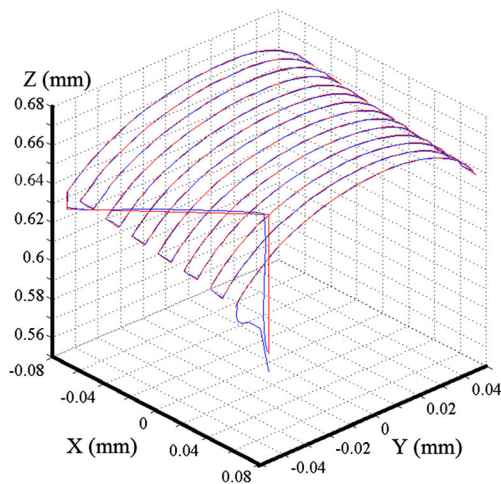


Fig. 9 Simulated motion curve of table for moving on turbine blade surface in SimMechanics and the desired curve obtained from the CAD model

four areas of trigonometric circle, the start and end angles of circle are calculated as follows:

$$\theta = \text{tg}^{-1}(J/I) : \begin{cases} f0 \leq \theta < \pi/2 \Rightarrow \theta = \theta \\ \text{if } \pi/2 \leq \theta < 3\pi/2 \Rightarrow \theta = \theta + \pi \\ \text{if } 3\pi/2 \leq \theta < 2\pi \Rightarrow \theta = \theta + 2\pi \end{cases} \quad (16)$$

The fourth step calculates β and α from Eqs. (9) and (13), respectively. The fifth step in Fig. 4, $\theta = \theta_s$, indicates the interpolation step of the algorithm. The details of this step,

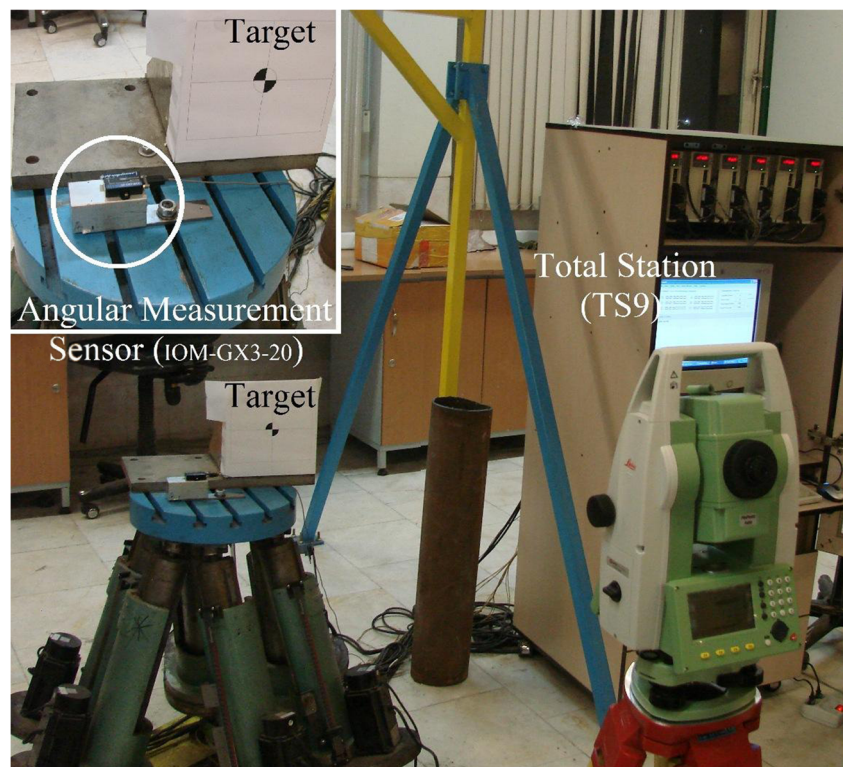
moreover, are presented in Fig. 4. In this step, considering the predefined acceleration, 50 mm/s^2 in this study, the accelerator unit of the table correlates the velocity of the table to the velocity defined by operator, and then, platform moves with constant velocity, and finally, the accelerator unit of the table acts to reduce the velocity of the moving platform. Nonlinear error analysis is performed for all the steps of trapezoidal velocity profile. Feed rate is changed by Eq. (11) to obtain a proper S and control kinematic error. Since this circular movement should be combined with the rotation of the table, calculation of interpolation points is performed regarding the circle center and after calculating next point of radius normal vector at the same point, and three Euler angles are obtained by relation (15).

5 Tool path programming for the motion of the table on a freeform surface

To investigate accuracy of interpolating algorithm while table motion on a freeform path, a CAD model with freeform characteristic is needed. For this purpose, Turbine blade of a gas turbine, length of 14 cm and width of 10 cm, is modeled by Imager 5006 (ZF), and its CAD model is extracted by importing ASCII file to CATIA (Fig. 5).

Due to the large curvature of the turbine blade mentioned in Fig. 5, when the rotation of the table is taken into account, using this model is not appropriate to verify the algorithm.

Fig. 10 Primary arrangements for experimental test



This, however, is thanks to the fact that the rotation of platform exceeds the workspace borders of the table in this condition. Therefore, by magnification of turbine blade with high curvature on X axis, the turbine blade with low curvature is obtained (Fig. 6).

6 Simulation study

In order to simulate the motion on the mentioned freeform surface in MATLAB, the CAD model of hexapod table is developed in SolidWorks and imported into the SimMechanics environment of MATLAB software. Figure 7 illustrates the Simulink model of hexapod table.

Figure 8 presents the simulated model for hexapod table in SimMechanics environment of MATLAB with its control block diagram. In len block, the position of the table is determined using six parameters of positions and Euler angles of the platform center, which is the input of the software. The output of this block diagram is entered to next block diagram which is related to the control unit of the hexapod table. The output of control system which determines displacement of the pod is entered to plant block. Within this block, there are all different kinds of modeled joints for the table. This model has two output blocks, namely, Simout and Scope. Passing trajectory of the center of the platform is obtained using Simout output, and then, the motion error is calculated by comparing Simout output with that of turbine blade surface.

Six parameters related to the position and Euler angles of the platform center in different points on freeform surface are considered as the inputs of len block. By importing CAD model of the turbine blade with high curvature as a freeform surface to the program written in C#.Net, these points are obtained by the aid of the algorithm developed in this paper. Since the rotation of the table exceeds the borders of workspace in this condition, the rotation of platform is neglected in this part of the simulation, and the results of the simulation are shown in Fig. 9. Blue curve of Fig. 9 is the

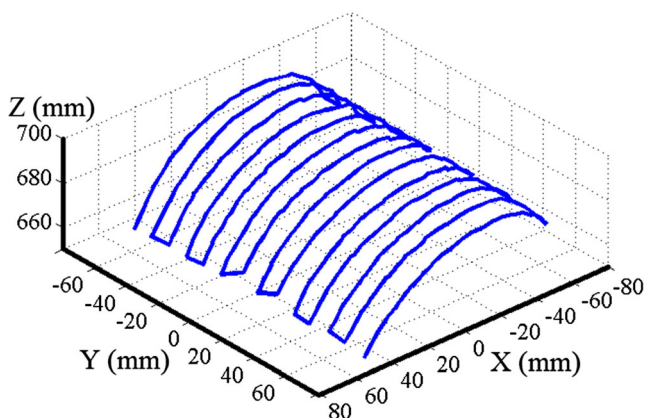


Fig. 11 Path of turbine blade surface with high curvature

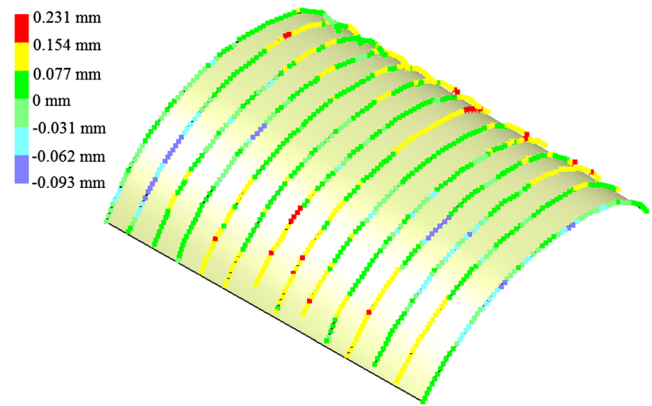


Fig. 12 Table motion error on turbine blade with high curvature, experimental test

simulated motion curve of the platform center to move in motion on the turbine blade surface, and the red curve corresponds to the desired curve on the turbine blade which is obtained from the CAD model. Since the motion of hexapod table is considered completely ideal in simulation, average error of the two paths is obtained less than 0.01 mm. This, however, is because of the fact that the control system of hexapod mechanism sends pulses at intervals of 0.1 s. Low error rates obtained in this setting confirm that the algorithm is correct.

7 Experimental test

For performing experimental measurement on interpolated points, Total Station camera, model TS9, is used. After receiving coordinate of two points in the space, this camera arranges its coordination, and then, automatically measures its distance from the target by sending a laser beam to it. Afterward, using its rotational axis in cylindrical coordinates, the camera acquires the desired position and automatically shows it in Cartesian coordinate system. When the machine table is rotating, IOM-GX3-20 sensor is utilized to measure its

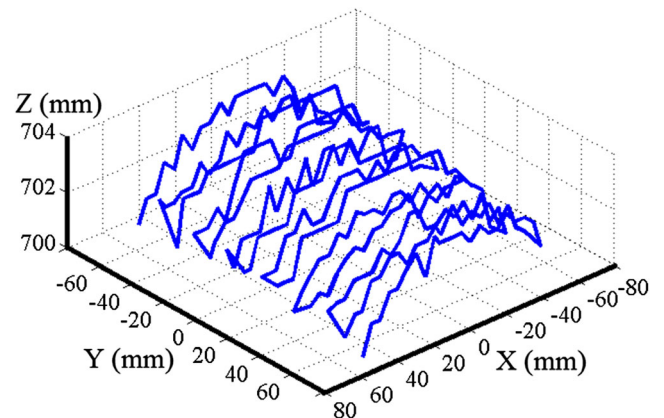
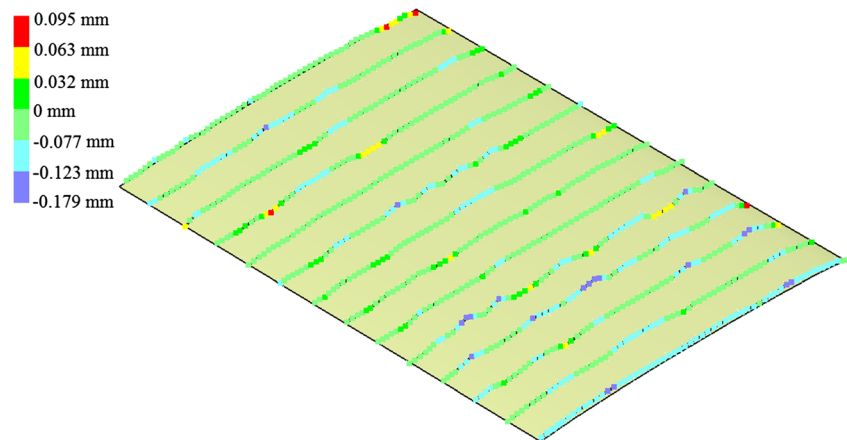


Fig. 13 Path of turbine blade surface with low curvature

Fig. 14 Table motion error on turbine blade with low curvature, experimental test



angle. This sensor saves the table angle in an Excel file. The experimental setup is shown in Fig. 10. After running the Human Machine Interpolation (HMI) software in the hexapod control system, TRAJECSIA, a pause command is used. In this condition, hexapod table which is moving from one interpolated point to another stops and waits for operator's command. When the machine is in stop mode, position of the target is sensed by camera, and this is repeated for next move, and consequently, moving path of platform is obtained in this way. Figure 11 shows motion of platform center using obtained points from experimental test by Total Station camera and for turbine blade with high curvature.

In order to check the accuracy of hexapod motion, position of platform center obtained by experimental test in movement on turbine blade surface is imported to CATIA software in ASCII file. According to Fig. 12, the error obtained by CATIA software for motion on turbine blade surface with high curvature is equal to 0.324 mm. Clearance between the gears, spherical and universal joint clearance, and errors resulted from assembling are the causes of these errors.

For turbine blade with low curvature, it is possible to expect that the rotation of the table satisfies workspace limitations of hexapod table respecting angular displacement. In this case, therefore, table rotation is taken into consideration. Table motion for points obtained from experimental test for turbine plate with low curvature is illustrated in Fig. 13.

Graphical check for error in CATIA software for navigating of turbine blade surface with low curvature indicates that the error is 0.274 mm which is shown in Fig. 14. When the table rotates and moves at the same time, reduction of error rate for 0.05 mm shows the effect of spherical joints on mechanism's clearance. This, however, is because that the increase of table rotation decreases the clearance and the motion error rate.

The difference between the results of the experimental test and simulation results can be attributed to the clearance of spherical joints. It should also be noted that the clearance existing in actuators and servos could have contributions in the overall difference of the results of both the methods.

8 Conclusions

In this paper, a comprehensive algorithm for tool path programming of hexapod table is developed. Using C#.Net, this algorithm is developed based on both circular motion and rotation of the table. The algorithm, moreover, has the capability of checking nonlinear motion error and keeps it in a controlled limit as well. This algorithm by using rotational capability of the table makes it possible to move with a higher degree of freedom. As a case study for motion of table on freeform surfaces, two different turbine blades with high and low curvatures, which respectively lead to the rotational and nonrotational motion of the table, are investigated via both simulation and experimental methods. Motion error resulted from simulation is less than 0.01 mm which proves the accuracy of the developed algorithm. Motion errors resulted from experimental tests for motion on freeform surfaces are 0.324 and 0.274 mm for turbine blade surfaces with high and low curvatures, respectively. The differences between these results indicate effects of clearance of universal joint on performed experimental tests.

References

- Zhang D (2010) Parallel robotic machine tools. Springer, Oshawa
- Chi Z, Zhang D, Xia L, Gao Z (2013) Multi-objective optimization of stiffness and workspace for a parallel kinematic machine. *Int J Mech Mater Des* 9:281–293
- Pedrammehr S, Mahboubkhah M, Khani N (2013) A study on vibration of Stewart platform-based machine tool table. *Int J Adv Manuf Technol* 65:991–1007
- Pedrammehr S, Mahboubkhah M, Chalak Qazani MR, Rahmani A, Pakzad S (2014) Forced vibration analysis of milling machine's hexapod table under machining forces. *Stroj Vestn-J Mech E* 60: 158–171
- Gao Z, Zhang D (2014) Simulation driven performance characterization of a spatial compliant parallel mechanism. *Int J Mech Mater Des*. doi:10.1007/s10999-014-9243-4

6. Jia Z-Y, Lin S, Liu W (2010) Measurement method of six-axis load sharing based on the Stewart platform. *Measurement* 43:329–335
7. Wang Z, Li Z, He J, Yao J, Zhao Y (2013) Optimal design and experiment research of a fully pre-stressed six-axis force/torque sensor. *Measurement* 46:2013–2021
8. Dasgupta B, Mruthyunjaya TS (1998) Singularity-free path planning for the Stewart platform manipulator. *Mech Mach Theory* 33: 711–725
9. Shaw D, Chen YS (2000) Cutting path generation of the Stewart platform-based milling machine using an end-mill. *Int J Prod Res* 39: 1367–1383
10. Merlet JP (2001) A generic trajectory verifier for the motion planning of parallel robots. *Trans ASME* 123:509–515
11. Pugazhenth S, Nagarajan T, Singaperumal M (2001) Optimal trajectory planning for a hexapod machine tool during contour machining. *P I Mech Eng C-J Mec* 216:1247–1257
12. Peidong W, Changlin W (2008) Motion planning and coupling analysis based on 3-RRR(4R) parallel mechanism. *Int J Mech Mater Des* 4:325–331
13. Dash AK, Chen IM, Yeo SH, Yang G (2005) Workspace generation and planning singularity-free path for parallel manipulators. *Mech Mach Theory* 40:776–805
14. Afroun M, Chettibi T, Hanchi S (2006) Planning optimal motions for a DELTA parallel robot. *Proceedings of the 14th IEEE Mediterranean Conference on Control and Automation*, Ancona, 28–30 June 2006
15. Afroun M, Chettibi T, Hanchi S, Dequidet A, Vermeiren L (2008) Optimal motions planning for a GOUGH parallel robot. *IEEE 16th Mediterranean Conference on Control and Automation Congress Centre*, Ajaccio, 25–27 June 2008
16. Harib KH, Sharif Ullah AAM, Hammami A (2007) A hexapod-based machine tool with hybrid structure: kinematic analysis and trajectory planning. *Int J Mach Tools Manuf* 47:1426–1432
17. Li Z (2000) Reconfiguration and tool path planning of hexapod machine tools. PhD thesis, New Jersey Institute of Technology
18. Jinsong W, Zhonghua W, Tian H, Whitehouse DJ (2002) Nonlinearity for a parallel kinematic machine tool and its application to interpolation accuracy analysis. *Sci China Ser A* 45:625–637
19. Zheng K, Gao J, Zhao Y (2005) Path control algorithms of a novel 5-DOF Parallel machine tool. *Proceedings of the IEEE International Conference on Mechatronics and Automation*, Ontario, 1381–1385
20. Chalak Qazani MR, Pedrammehr S, Rahmani A, Danaei B, Ettefagh MM, Khani Sheykh Rajab A, Abdi H (2014) Kinematic analysis and workspace determination of hexarot—a novel 6-DOF parallel manipulator with a rotation-symmetric arm system. *Robotica*. doi:10.1017/S0263574714000988
21. Chalak Qazani MR, Pedrammehr S, Rahmani A, Shahryari M, Khani Sheykh Rajab A, Ettefagh MM (2014) An experimental study on motion error of hexarot parallel manipulator. *Int J Adv Manuf Technol* 72:1361–1376
22. Heisel U, Gringel M (1996) Machine tool design requirements for high speed machining. *Ann CIRP* 45:389–392
23. Harib K, Srinivasan K (2003) Kinematic and dynamic analysis of Stewart platform-based machine tool structures. *Robotica* 21:541–554
24. Li Y-J, Wang G-C, Zhang J, Jia Z-Y (2012) Dynamic characteristics of piezoelectric six-dimensional heavy force/moment sensor for large-load robotic manipulator. *Measurement* 45:1114–1125
25. Pedrammehr S, Mahboubkhah M, Pakzad S (2011) An improved solution to the inverse dynamics of the general Stewart platform. *Proceedings of the 2011 I.E. International Conference on Mechatronics*, ICM 2011, 5971317:392–397
26. Pedrammehr S, Mahboubkhah M, Khani N (2012) Improved dynamics equations for the generally configured Stewart platform manipulator. *J Mech Sci Technol* 26:711–721
27. Nanfarra F, Uccello T, Murphy D (1995) *The CNC workbook*. Addison-Wesley Publishing Company, MA